

# Thermionic electron emission microscopy of metal-oxide multilayers on tungsten

J. M. Vaughn  
C. Wan  
K. D. Jamison  
M. E. Kordesch

*Thick (200-nm) layers of reactively sputtered BaO and Sc<sub>2</sub>O<sub>3</sub> on tungsten foil are imaged with thermionic electron emission microscopy (ThEEM). The scandia films are observed to show what we have named the “window effect,” i.e., apparent electron transparency in the ThEEM image, showing the underlying structure of the polycrystalline W foil.*

## Introduction

Thermionic cathodes are used in many industrial vacuum electronic applications. Vacuum tubes for high-frequency or high-power applications are one example (e.g., see [1]). The emission properties of thermionic electron sources in vacuum devices are often “improved” by the addition of oxide coatings on the metal cathode surface [2, 3]. The explanation of the improvement is usually based on the creation of a surface dipole. BaO is often used. The oxygen atom (ion) is embedded in the tungsten surface, and the Ba atom (ion) is outermost at the surface-vacuum interface [4–6]. Practical cathodes, however, are made with bulk powder loading of a porous tungsten plug [7]. Some are made by spray coating with a layer on the order of 65  $\mu\text{m}$  [8]. The monolayer surface dipole structure is thought to develop as the cathode is heated and “activated” [9].

Recent experimental [10, 11] and theoretical [12] studies have suggested that multilayer oxides on the order of 10 nm can also reduce the work function of a metal. The work function is reduced by the alteration of the buried metal-oxide interface rather than at the oxide-vacuum surface.

In this paper, we demonstrate that 200- to 400-nm-thick oxide layers can increase the electron yield from a heated tungsten surface. The thermionic electron emission microscopy (ThEEM) images of the oxide layers on tungsten show a unique “window”-like view of the tungsten grain structure through the oxide. No structures resulting from

the oxide are resolved in the image. The window effect is proposed to result from a reduced interfacial energy barrier at the W-Sc<sub>2</sub>O<sub>3</sub> interface and the electrical conductivity of Sc<sub>2</sub>O<sub>3</sub> at high temperatures ( $>1,100$  K).

## Experimental

The microscope used is a Bauer–Telleps style emission microscope [13] in the vertical inverted “Y” configuration. The acceleration voltage used is 7 kV with a 4-mm working distance. The specimen is heated from the back by electron bombardment. The sample temperature is measured with an optical pyrometer [14, 15]. We measure brightness temperature  $T_b = \varepsilon T_{\text{true}}$ , where  $\varepsilon$  is the emissivity. The emissivity of our composite surfaces is unknown. The oxide layers are deposited by reactive sputtering in a separate chamber. Shadow masks are used, which allow deposition of 100  $\mu\text{m} \times 100 \mu\text{m}$  or 25  $\mu\text{m} \times 25 \mu\text{m}$  squares of oxide on the tungsten surface, to provide image contrast and to identify the deposited oxide layer (by size) in the image. The film thickness is obtained directly from a quartz crystal thickness monitor. The values are minimum thickness values. The samples are exposed to air between depositions and also before introduction into the microscope. The samples are degassed by several heating cycles and then repeatedly heated until the window effect is observed.

Emission current is measured by using a Faraday cup in the center of the channel plate electron multiplier. The exact location of the current measurement can be established. The current is recorded with a Keithley 488 picoammeter. The current, brightness temperature (which can also be denoted by  $K_b$ , i.e., units of Kelvin), and image are stored together using a LabVIEW program. Note that

Digital Object Identifier: 10.1147/JRD.2011.2159423

© Copyright 2011 by International Business Machines Corporation. Copying in printed form for private use is permitted without payment of royalty provided that (1) each reproduction is done without alteration and (2) the Journal reference and IBM copyright notice are included on the first page. The title and abstract, but no other portions, of this paper may be copied by any means or distributed royalty free without further permission by computer-based and other information-service systems. Permission to republish any other portion of this paper must be obtained from the Editor.

0018-8646/11/\$5.00 © 2011 IBM

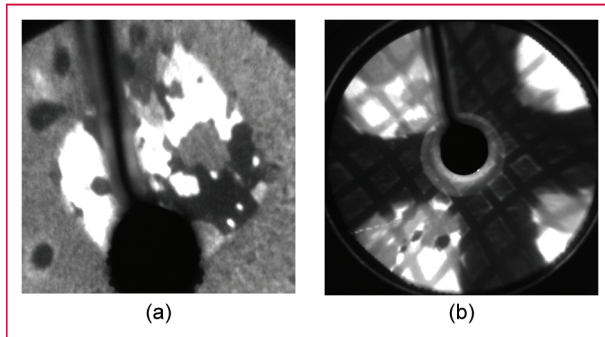


**Figure 1**

ThEEM images of (a) the  $\text{Sc}_2\text{O}_3$   $100\ \mu\text{m} \times 100\ \mu\text{m}$  square on a W foil at 1,191  $\text{K}_b$  (brightness  $T$ ) and of (b) the  $\text{Sc}_2\text{O}_3$   $100\ \mu\text{m} \times 100\ \mu\text{m}$  squares with BaO  $25\ \mu\text{m} \times 25\ \mu\text{m}$  squares on top. ( $T_b = 1,303\ \text{K}_b$ . Heating cycle: 18.)

$K_b = \varepsilon \times K_{\text{true}}$ , and  $\varepsilon < 1$ . In order to make the current measurements, the emissive square is moved onto the Faraday cup in the image plane by shifting the image with deflector coils located in the projector side of the ThEEM microscope. The sample itself remains stationary. The magnification is not changed. The square itself is a measure of the area on the sample surface.

## Results

**Figure 1(a)** shows a ThEEM image at a brightness temperature of 1,191  $\text{K}_b$  of a 200-nm-thick  $\text{Sc}_2\text{O}_3$  film deposited on tungsten. The  $100\ \mu\text{m} \times 100\ \mu\text{m}$  square looks like a transparent window on the W surface. The grain structure of the W foil can be observed through the window. **Figure 1(b)** shows a ThEEM image at 1,303  $\text{K}_b$  of a two-layer BaO on  $\text{Sc}_2\text{O}_3$  on the W structure. In this image, the window effect extends through two 200-nm-thick oxide layers. The small squares show further electron-yield enhancement relative to the narrow grid of  $\text{Sc}_2\text{O}_3$  on W. The grid can be observed between the bright BaO squares. The electron yield shows clear dependence on the oxide layers. The underlying W grain structure also shows variations. Not all of the small BaO squares are bright (high yield). Those that are situated on  $\text{Sc}_2\text{O}_3$  but on a nonemissive W grain, such as the two at the top left of the image, are not as bright as others. The BaO squares that are not on  $\text{Sc}_2\text{O}_3$  show little or no emission relative to the other two-layer structures. BaO squares that are half on and half off the  $\text{Sc}_2\text{O}_3$  square show an electron-yield enhancement only in the “on” portion. It should be noted from the image that the BaO squares are stable and do not diffuse or “melt” or otherwise decay at the temperatures used in this study.

**Figure 2** shows the fit of the electron yield (measured with a Faraday cup in the image plane) as a function of brightness

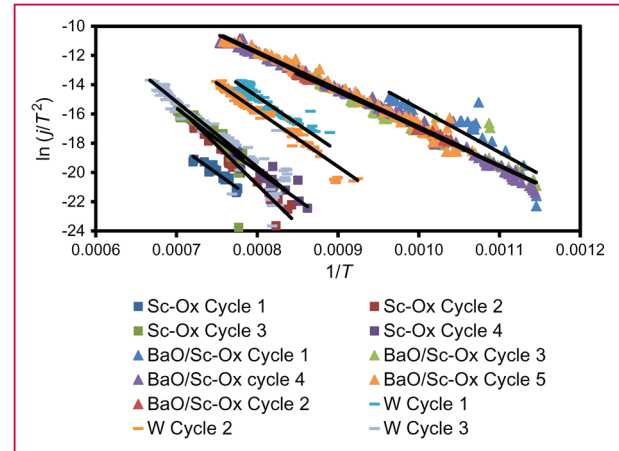


**Figure 2**

$\ln(j/T^2)$  versus  $1/T$  for BaO on  $\text{Sc}_2\text{O}_3$  on W (triangles),  $\text{Sc}_2\text{O}_3$  on W (squares), and W (dashes).

temperature to the Richardson–Dushman equation [16]. A fit for tungsten foil is also included. The work function is not directly measured in our experiment. A multicomponent entity, which we call the “work function,” is derived from the  $j$  versus  $T$  data fits to the Richardson–Dushman equation. Here,  $j$  is the current density. The “work function” is proportional to the slope of the  $\log(j/T^2)$  versus  $1/T$  curves shown in Figure 2.

The phrase “work function” (with surrounding quotation marks, “ ”) can only be estimated in our experiments, partly due to the systematic error that occurs measuring the brightness temperature versus the true temperature. The “work function” reduction (electron-yield enhancement) due to the added oxide layers can be measured because it is a relative shift in the “work function” values. Because the value for emissivity is less than 1, the “work function” values can be shifted to account for the systematic error in temperature. The work function value for a W foil measured in ThEEM is too low. By shifting the value to the known (average) value for the tungsten surface, a comparison with other types of work function reduction measurements and calculations can be made more easily. We have determined that the correction for the emissivity and other factors on tungsten is approximately 0.76. Comparison of the pyrometer reading and a C-type thermocouple for a tungsten foil confirms that the value of  $\varepsilon$  for W in our experiment is in the range of 0.74–0.76. This method should not be applied to the scandium foil or  $\text{Sc}_2\text{O}_3$  surfaces. For our measurements, the correction implies an emissivity value greater than 1. If the values for the scandium foil or  $\text{Sc}_2\text{O}_3$  surfaces are acknowledged to represent a combination of energy barriers and other effects not strictly defined as a work function, some comparisons can be made. In that case, it is necessary

**Table 1**  $\Phi$  comparison for thin-film cathodes, where  $\Phi$  is the work function. The last two columns represent  $\Phi/0.758$  and  $\Phi/1.606$ , respectively.

Coating	$\Phi$ (eV) (measured)	$\Phi/0.758$	$\Phi/1.606$
Sc foil	$5.6 \pm 1.9$	—	3.50
W foil	$3.5 \pm 0.3$	4.55	—
W foil + Sc <sub>2</sub> O <sub>3</sub>	$3.8 \pm 0.6$	4.97	2.35
W foil + Sc <sub>2</sub> O <sub>3</sub> + BaO	$2.3 \pm 0.2$	2.99	1.41

to use a correction value of 1.6 to shift the measured value of a Sc foil to the value reported in the literature. This is done for comparison only, i.e., the value of 5.6 eV is consistent with the other values to within the error of the Richardson-Dushman fitting method. Some values obtained from the Richardson-Dushman equation fits are given in **Table 1**.

## Discussion

The clear electron-yield enhancement due to the thick (~200–400 layers) oxides is shown in Figure 1(a) and 1(b). There is a difference between an electron-yield enhancement due to the reduction of an interfacial energy barrier and the reduction of the surface-vacuum energy barrier. This distinction is essential to the understanding of the action of thick oxide layers in thermionic emission.

The work function is strictly defined as the energy barrier at the solid-vacuum interface. Our oxide layers are not monolayers on a metal. We do not directly measure the surface dipole or surface energy barrier. The “work function” value derived from the  $I$  versus  $T$  data may include contributions from the work function of the underlying W grain, the interfacial energy barrier at the W-Sc<sub>2</sub>O<sub>3</sub> interface, and the surface energy barrier. For BaO-Sc<sub>2</sub>O<sub>3</sub>-W layers, there may also be a contribution due to an interfacial barrier at the BaO-Sc<sub>2</sub>O<sub>3</sub> interface. **Figure 3** provides a schematic explanation of the information that we obtained from the ThEEM images.

The starting point in understanding the images in Figure 1(b) is to realize that at the same temperature, under identical conditions, the work function of all of the BaO squares must be the same. The BaO directly on tungsten and the BaO on Sc<sub>2</sub>O<sub>3</sub> must have the same surface-vacuum interfacial energy barrier (the strict interpretation of the work function). There can be no interaction with W or Sc<sub>2</sub>O<sub>3</sub> at the BaO surface because these materials are at least 200 nm below the surface. In Figure 3, the work function of BaO is represented as a thick green vertical line in the diagrams (the same size in both places). In addition, the

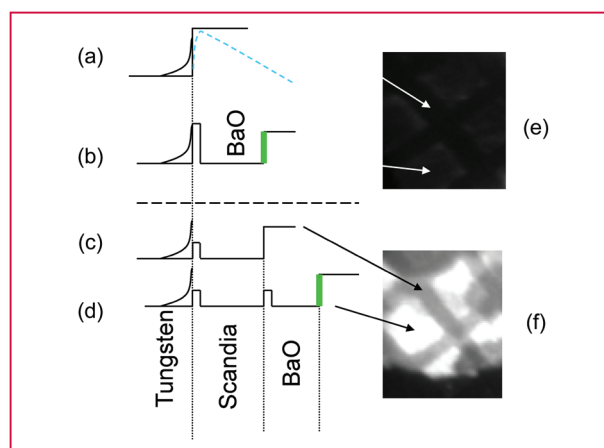


**Figure 3**

Schematic explanation. (a) Tungsten surface. Only the energy region from Fermi to vacuum levels is shown. On the left is the Fermi distribution tail due to heating. The blue dashed line shows the effect of the applied field, which reduces the surface barrier. The electric field also penetrates the oxide layers but is not shown in (b)–(d) for clarity. The image of the tungsten surface is shown in (e), which is indicated by an arrow pointing at the space between the BaO squares. (b) Schematic diagram of the W-BaO interfacial barrier. The BaO work function is shown in (e), which is indicated by an arrow pointing at a BaO square. (c) Sc<sub>2</sub>O<sub>3</sub> on W. The interfacial barrier is unknown but less than BaO-W. The work function is also unknown. The electron yield is greater than for BaO at the same  $T$ ; thus, the combined interfacial energy barrier and work function must be less than for BaO. The image of Sc<sub>2</sub>O<sub>3</sub> on W is shown in (f), and the arrow points to the space between BaO squares. (d) BaO on Sc<sub>2</sub>O<sub>3</sub> on W. The interfacial barriers are shown. The thick green line at the surface of the BaO, which indicates the work function of BaO, must be the same as that for (b). As a consequence, the improved electron yield is due to interfacial barrier reductions. The image of BaO on Sc<sub>2</sub>O<sub>3</sub> on W is shown in (f), and the arrow points to BaO squares on Sc<sub>2</sub>O<sub>3</sub> on W. (e) and (f) are taken from Figure 1(b).

same BaO square can show different electron yields if it is partially on or off a Sc<sub>2</sub>O<sub>3</sub> square.

Because the electron yield from W-BaO is less than that from W-Sc<sub>2</sub>O<sub>3</sub>-BaO, the yield increase must be due to changes in interfacial energy barriers. It cannot be due to a change in the BaO work function. The evidence for this conclusion is shown in **Figure 3(b)** and **3(d)**. While the numerical “work function” values measured in the ThEEM are not accurate in an absolute sense, the values measured in the microscope are internally consistent and can be compared. The value for the “work function” change for the W-Sc<sub>2</sub>O<sub>3</sub>-BaO relative to the W-Sc<sub>2</sub>O<sub>3</sub> surface is 1.5 eV. The values that we derive from the fit of the electron yield from thick oxide multilayers to the Richardson-Dushman equation include *sequential* interfacial energy barriers and a surface barrier.

Depending on how the change in “work function” is interpreted, the W surface covered with Sc<sub>2</sub>O<sub>3</sub> now has an

effective work function of 3.8 eV. This is an *increase* of 0.3 eV from the work function of W measured in the microscope, or a 0.42-eV *increase* from the accepted value for tungsten, i.e., 4.97 eV compared with 4.55 eV [17]. There is a decrease in the W-Sc<sub>2</sub>O<sub>3</sub> “work function” only if the shifted scandium values are used. Scandium oxide has a bandgap of 5.5 eV or more and an unknown electron affinity [18, 19]. The measured value of the Sc foil (with a native oxide) may be correct. The strict interpretation of work function for a thick scandium oxide layer would place the work function value above 5.5 eV. However, the experimental evidence in Figure 1(a) seems to contradict the “work function” for W-Sc<sub>2</sub>O<sub>3</sub> derived from the *I* versus *T* data.

An alternative to the “surface dipole” explanation is clearly needed. Models of cathode function in the past have not separated the role of scandium oxide from the tungsten or barium oxide. The “semiconductor model” of Wright and Woods [20] and the later adaptation by Raju and Maloney [21] come closest to our model cathodes. The semiconductor model assumes that the oxide layer behave as a semiconductor. Electron emission is from the conduction band of the oxide. Raju and Maloney postulate that both separate Sc<sub>2</sub>O<sub>3</sub> and BaO-Sc<sub>2</sub>O<sub>3</sub> (alloy) layers form and that the layers are thick (100- $\mu$ m total, 0.4–0.5- $\mu$ m-thick “active layers”). The “semiconductor” aspect of this model is the inclusion of a small reduction of the metal-oxide interfacial energy barrier due to penetration of the electric field through the oxide layer to the W surface [represented in Figure 3(a) as the blue dashed line]. Therefore, the model includes a surface barrier reduction at the oxide-vacuum interface due to band bending and another at the W-oxide interface due to the Schottky effect. Patches of emissive material with different surface areas and different work functions are *parallel* interfacial energy barriers. These models do not apply to the two-layer *sequential* interfacial energy barriers observed in Figure 1(b). In a sequential arrangement of energy barriers, the largest barrier determines the total yield. In parallel energy barriers, the smaller barrier dominates at lower temperatures. An example of electron emission through parallel barriers would be the image in Figure 1(a), where the W surface outside the Sc<sub>2</sub>O<sub>3</sub> square has a different electron yield than the Sc<sub>2</sub>O<sub>3</sub> square itself. Parallel energy barriers might also be applicable to the different W grains observed in the Sc<sub>2</sub>O<sub>3</sub> square.

In addition to barrier reductions, the window effect requires that the oxides be conductive. The physical properties of scandium oxide are not well known. The properties of bulk Sc<sub>2</sub>O<sub>3</sub> at high temperature, including conductivity [22, 23] and structure changes, have been reported [24]. Scandium oxide is an ionic conductor, both by oxygen and scandium motions, and both an n- and p-type semiconductor [23]. The various conduction mechanisms are a function of oxygen content. The conductivity of

Sc<sub>2</sub>O<sub>3</sub> is indirectly a function of temperature due to oxygen vacancies introduced by heating. Scandium is a 3+ ion in scandium oxide, and there is no other monovalent or divalent form of bulk scandium oxide. Oxygen vacancies can result in excess electrons in the oxide. Scandium oxide is considered a nonstoichiometric oxide because of oxygen vacancies. Structural changes begin as low as 673 K, and the nonstoichiometric form is stabilized with high temperature treatment [24]. Because we sputter-deposit our films, a disordered film structure is likely for the as-deposited scandium oxide [25]. Heating this disordered film may promote further oxygen vacancies in the film. Oxygen vacancies would increase the electronic conductivity at the high temperatures used to observe the window effect.

The scandium oxide layer at high temperature is considered a highly doped n-type semiconductor (with an unknown bandgap). The conventions used to describe thermionic emission in Schottky barrier contacts can be applied to the tungsten-scandium oxide interface [26]. The bottom of the scandium oxide conduction band would align with the Fermi level of the tungsten metal. There would be a small barrier of 0.1–0.2 eV that could be overcome by heating to the working temperature of the cathode, which is about 1,000 K. The window effect would be the result of electron emission from an electron-rich n-type semiconductor formed by the W-Sc<sub>2</sub>O<sub>3</sub> layer. The surface energy barrier would be equal to or slightly larger than the electron affinity of the scandium oxide [21]. The electron supply would come from the tungsten, pass through the scandium oxide, and exit over a surface barrier on the order of 2 eV. The value of 2 eV is consistent with scandium oxide-like materials (even at 300 K) [18] and the ThEEM image in Figure 1(a).

The electron concentration in BaO used by Wright and Woods was measured to be in the range of  $1 \times 10^{14} \text{ cm}^{-3}$  with a conductivity value of  $3 \times 10^{-2} (\Omega \cdot \text{cm})^{-1}$ . The electron concentration is a result of free Ba in BaO. The value is claimed by Wright and Woods to be consistent with the solubility of Ba in BaO. Values for other nonscantate oxide cathodes [27] are in agreement with the BaO data of Wright and Woods. The electron concentration in bulk scandia at 1,473 K is reported in [22, 23] to be in the range of  $10^{14} - 10^{19} \text{ cm}^{-3}$  as a function of decreasing oxygen partial pressure. This electron concentration is a result of free Sc in Sc<sub>2</sub>O<sub>3</sub>; in the same way, free Ba donates electrons in BaO. The bulk conductivity in this range is less than  $10^{-6} (\Omega \cdot \text{cm})^{-1}$ . The bulk conductivity of Sc<sub>2</sub>O<sub>3</sub> is lower than that reported for oxide cathodes. If thin-film Sc<sub>2</sub>O<sub>3</sub> were more susceptible to oxygen depletion, the conductivity of thin-film Sc<sub>2</sub>O<sub>3</sub> might be closer to the conductivity of oxide cathodes. If the Sc<sub>2</sub>O<sub>3</sub> and BaO conductivity values in the cathode are comparable, the conductivity does not play a limiting role in the electron yield. The window effect

is then most probably due to an interfacial energy barrier reduction.

The changes in scandium oxide conductivity measured in [22] are the result of heating, which removes some oxygen from the scandium oxide. The scandium oxide structure is stabilized by the removal of oxygen. The stabilization of a conductive form of scandium oxide is a plausible explanation for part of the function of scandium oxide in cathodes. Increased conductivity in  $\text{Sc}_2\text{O}_3$  may also be induced by the current passing through the scandium oxide during thermionic emission. The current and the acceleration voltage could provide electrons with sufficient energy to further deplete the oxide of oxygen. Similar effects have been reported for other oxides [28, 29].

## Conclusion

The electron-yield enhancement caused by thick scandium oxide layers on tungsten is attributed to a reduced interfacial energy barrier at the W- $\text{Sc}_2\text{O}_3$  interface. A surface dipole effect is excluded. Based on the observation of a fully electron transparent thick layer that appears as a window in the ThEEM image, we have concluded that  $\text{Sc}_2\text{O}_3$  and BaO are conductors at cathode operation temperatures. The improvement caused by  $\text{Sc}_2\text{O}_3$  addition to the oxide cathodes is due to a reduced interfacial energy barrier at the W- $\text{Sc}_2\text{O}_3$  interface relative to scandia-free oxide-coated cathodes. A secondary benefit of scandia additions is increased conductivity at high temperatures.

## Acknowledgment

This work was supported by Nanohmics, Inc. through the Air Force Office of Scientific Research under Contract FA9550-09-C-0085.

## References

1. R. J. Barker, J. H. Booske, N. C. Luhmann, Jr., and G. S. Nusinovich, *Modern Microwave and Millimeter-Wave Power Electronics*. Piscataway, NJ: IEEE Press, 2005.
2. H. Friedenstein, S. L. Martin, and G. L. Munday, "The mechanism of the thermionic emission from oxide coated cathodes," *Rep. Prog. Phys.*, vol. 11, pp. 289–341, 1947.
3. S. Yamamoto, "Fundamental physics of vacuum electron sources," *Rep. Prog. Phys.*, vol. 69, no. 1, pp. 181–232, Jan. 2006.
4. V. Vlahos, Y. L. Lee, J. H. Booske, D. Morgan, L. Turek, M. Kirshner, R. Kowalczyk, and C. Wilsen, "Ab initio investigation of the surface properties of dispenser B-type and scandate thermionic emission cathodes," *Appl. Phys. Lett.*, vol. 94, no. 18, article no. 184102, May 2009.
5. K. L. Jensen, D. W. Feldman, N. A. Moody, and P. G. O'Shea, "A photoemission model for low work function coated metal surfaces and its experimental validation," *J. Appl. Phys.*, vol. 99, no. 12, article no. 124905, Jun. 2006.
6. K. L. Jensen, "Exchange-correlation, dipole, and image charge potentials for electron sources: Temperature and field variation of the barrier height," *J. Appl. Phys.*, vol. 85, no. 5, pp. 2667–2680, Mar. 1999.
7. Y. Wang, J. Wang, W. Liu, K. Zhang, and J. Li, "Development of high current density cathodes with scandia doped tungsten powders," *IEEE Trans. Electron Devices*, vol. 54, no. 5, pp. 1061–1070, May 2007.
8. A. N. H. Al-Ajili, A. K. Ray, A. K. Hassan, S. N. B. Hodgson, and C. J. Goodhand, "Dielectric properties of activated oxide emission materials," *Mater. Lett.*, vol. 57, no. 2, pp. 513–517, Dec. 2002.
9. D. den Engelsen and G. Gaertner, "Model of dopant action in oxide cathodes," *Appl. Surf. Sci.*, vol. 251, no. 1–4, pp. 50–58, Sep. 2005.
10. L. Giordano, M. Baistrocchi, and G. Pacchioni, "Bonding of Pd, Ag, and Au atoms on MgO(100) surfaces and MgO/Mo(100) ultra-thin films: A comparative DFT study," *Phys. Rev. B, Condens. Matter*, vol. 72, no. 11, article no. 115403, Sep. 2005.
11. E. V. Klimenko, L. N. Starovojtova, I. N. Zasimovich, and A. G. Naumovets, "Oxidation of barium on the surface of nanothick chromium oxide films grown on the (110) molybdenum surface," *Mat.-Wiss. u. Werkstofftech.*, vol. 40, no. 4, pp. 273–276, 2009.
12. S. Prada, U. Martinez, and G. Pacchioni, "Work function changes induced by deposition of ultrathin dielectric films on metals: A theoretical analysis," *Phys. Rev. B, Condens. Matter*, vol. 78, no. 23, article no. 235423, Dec. 2008, DOI: 10.1103/PhysRevB.78.235423.
13. W. Telieps and E. Bauer, "An analytical reflection and emission UHV surface electron microscope," *Ultramicroscopy*, vol. 17, no. 1, pp. 57–65, 1985.
14. J. M. Vaughn, K. D. Jamison, and M. E. Kordesch, "Photoelectron- and thermionic- emission microscopy of barium/scandium thin films on tungsten," in *Proc. Mater. Res. Soc., Symp. W*, vol. 1088, pp. 13–19, 2008.
15. J. M. Vaughn, K. D. Jamison, and M. E. Kordesch, "In situ emission microscopy of scandium/scandium-oxide and barium/barium oxide thin films on tungsten," *IEEE Trans. Electron Devices*, vol. 56, no. 5, pp. 794–798, May 2009.
16. S. Dushman, "Thermionic emission," *Rev. Mod. Phys.*, vol. 2, no. 4, pp. 381–476, Oct.–Dec. 1930.
17. H. B. Michaelson, "The work function of the elements and its periodicity," *J. Appl. Phys.*, vol. 48, no. 11, pp. 4729–4733, Nov. 1977.
18. X. Bai, "Growth and characterization of IIIB-nitride semiconductors and devices," Ph.D. dissertation, Ohio Univ., Athens, OH, 2000.
19. J. Robertson, "Band offsets of wide bandgap oxides and implications for future electronic devices," *J. Vac. Sci. Technol. B, Microelectron. Nanometer Struct.*, vol. 18, no. 3, pp. 1785–1791, May 2000.
20. D. A. Wright and J. Woods, "The emission from oxide-coated cathodes in an accelerating field," *Proc. Phys. Soc. B*, vol. 65, no. 2, pp. 134–148, Feb. 1952.
21. R. S. Raju and C. E. Maloney, "Characterization of an impregnated scandate cathode using a semiconductor model," *IEEE Trans. Electron Devices*, vol. 41, no. 12, pp. 2460–2467, Dec. 1994.
22. Z. S. Volchenkova and V. M. Nedopekin, "Electrical conductivity of  $\text{Sc}_2\text{O}_3$ ," *Inorganic Mater.*, vol. 11, no. 8, pp. 1205–1208, 1975.
23. Z. S. Volchenkova and V. M. Nedopekin, "Thermoelectric power in scandium oxide," *Sov. Electrochem.*, vol. 26, no. 6, pp. 666–668, 1990.
24. A. E. Solov'eva, "Phase inversion in polycrystalline scandium oxide," *Refractories Ind. Ceram.*, vol. 30, no. 5/6, pp. 357–360, 1989, DOI: 10.1007/BF01281509.
25. M. F. Al-Kuhaili, "Optical properties of scandium oxide films prepared by electron beam evaporation," *Thin Solid Films*, vol. 426, no. 1/2, pp. 178–185, Feb. 2003.
26. T. V. Blank and Y. A. Goldberg, "Mechanisms of current flow in metal–semiconductor ohmic contacts," *Semiconductors*, vol. 41, no. 11, pp. 1263–1292, Nov. 2007.
27. G. Gaertner, P. Janiel, and D. Raasch, "Direct determination of electrical conductivity of oxide cathodes," *Appl. Surf. Sci.*, vol. 201, no. 1–4, pp. 35–40, Nov. 2002.
28. O. Dulub, M. Batzill, S. Solovev, E. Loginova, A. Alchagirov, T. E. Madey, and U. Diebold, "Electron-induced oxygen desorption from the  $\text{TiO}_2$  (011)- $2 \times 1$  surface leads to

- self-organized vacancies,” *Science*, vol. 317, no. 5841, pp. 1052–1056, Aug. 2007.
29. D. A. Wright and J. Woods, “The decomposition of thin films on bombardment with slow electrons,” *Proc. Phys. Soc. B*, vol. 66, no. 12, pp. 1073–1086, Dec. 1953.

*Received September 21, 2010; accepted for publication February 14, 2011*

**Joel M. Vaughn** *Department of Physics and Astronomy, Ohio University, Athens, OH 45701 USA (jv218100@ohio.edu).*

**Congshang Wan** *Department of Physics and Astronomy, Ohio University, Athens, OH 45701 USA (cw140907@ohio.edu).*

**Keith D. Jamison** *Nanohmics, Inc., Austin, TX 78741 USA (kjamison@nanohmics.com).*

**Martin E. Kordesch** *Department of Physics and Astronomy, Ohio University, Athens, OH 45701 USA (kordesch@ohio.edu).*